X International Conference on Computational Methods in Marine Engineering
MARINE 2023
J. Garcia-Espinosa, L. González, J.E. Gutiérrez & B. Serván-Camas (Editors)

CFD analysis of the effect of frigate exhaustions on helicopter performances during on-board operations

MARINE 2023

R. Bardera[1], J.C. Matías-García[2*] and E. Barroso[3]

Instituto Nacional de Técnica Aeroespacial (INTA)
Ctra. Ajalvir, km 4.5
Torrejón de Ardoz, 28850 Madrid, Spain

[1]e-mail: barderar@inta.es, web page: http://www.inta.es
[2*]e-mail: matiasgjc@inta.es, web page: http://www.inta.es
[3]e-mail: barrosobe@inta.es, web page: http://www.inta.es

[*] Corresponding author: J.C. Matías-García, matiasgjc@inta.es

ABSTRACT

Helicopter recovery maneuvers on frigates can be a challenge for pilots. The aerodynamic interference between the frigate superstructure and the helicopter results in a complex airflow which causes an increase in the pilot's workload during the operations above the helideck. But the dangers are not just the presence of large areas of turbulent and detached flow. The interaction of the helicopter with the engine exhaust emissions from the frigate can affect pilot visibility and even the aircraft's performance. These high-temperature emissions coming out of the funnel can cause sudden changes in air density, affecting the performance of the aircraft turbine during the final phase of the maneuver. This paper aims to perform a numerical analysis using Computational Fluid Dynamics (CFD) to quantify the losses of performance that a helicopter may experience operating in the presence of frigate exhaust emissions. The study is performed on a Simplified Frigate Model, under different cases changing velocities and temperatures of the outlet gases, simulating a helicopter recovery maneuver from the stern. The results of the study show that temperatures can rise by up to 8ºC along the recovery path, which is higher than the 2ºC recommendation for the operations of helicopters around maritime structures. The increase in temperatures produces drops in engine performance and helicopter thrust of up to 2.4 %.

Keywords: CFD; Frigate; Helicopter; Recovery; Temperature; Thrust.

NOMENCLATURE

A	Surface of the helicopter main rotor [m^2]
EP	Engine power [kW]
H	High temperature outlet ($\eta = 1.70$)
K	Velocity coefficient
L	Low temperature outlet ($\eta = 1.30$)
L	Frigate length [m]

m	Constant value that depends of the helicopter engine ($m \sim 0.85$)
$\dot{m}$	Mass flow rate [$m^3\ s^{-1}$]
M	Medium temperature outlet ($\eta = 1.50$)
P	Air pressure [Pa]
T	Air temperature [K]
T_∞	Temperature of free-stream [K]
T_r	Rotor thrust [N]
T_s	Temperature of the outlet gases [K]
U_∞	Free stream velocity [m s^{-1}]
V_i	Induced velocity at the rotor plane [m s^{-1}]
V_e	Exit velocity of the outlet gases [m s^{-1}]
W	Vertical speed [m s^{-1}]
ΔEP	Engine power variations experienced
ΔT	Temperature variations
ΔT_r	Thrust variation
η	Non-dimensional temperature difference
θ	Increase of temperature in percentage with respect to the ambient temperature
ρ	Air density
CFD	Computational Fluid Dynamics
SFS2	Simple Frigate Shape 2
TTCP	Technical co-operation Program

1. INTRODUCTION

The flow around a frigate is complex and is dominated by high velocity gradients and turbulent intensity (Bardera, 2014). This leads to complex numerical simulations and often requires the use of wind tunnel tests with scale models. As the frigate aerodynamics, the problem of exhaust gases in marine ships was traditionally analyzed using scaled models in wind tunnels. Nowadays, as the computational capabilities have been increased a lot, the behavior of the exhaust gases from marine ship's chimney can be simulated numerically using CFD. The main reason for these kind of studies is that a frigate geometry above the deck is usually composed by tall mast and short chimneys. Then, the hot exhaust gases generated by its propulsion system can be retained close to the deck affecting ventilation, the crew and electronic devices on topside structures. For military frigates, it can also generate problems to weapon systems, increase the infrared signature, and interfere adversely with helicopter operations above the flight deck. The problem has worsened in recent years, as frigates use gas turbines instead diesel engines that generate exhaust flows with higher flow rates and temperatures. For these reasons it is essential to make predictions of the propagation trajectory and temperature distribution of the exhaust gas plume. This propagation is affected by different factors such as the outlet gases velocity, flow rate and temperature.

Dobrucali (2012) made a review of this kind of studies with a short summary of them. As indicated by Scott et al. (2015), when a helicopter is hovering inside the high temperature exhaust plume, the air density decreases and the engine power and thrust generated by the main rotor is reduced. Their simulations predicted air temperatures above the deck about 5ºC higher than the ambient. Although this increase may not seem too significant, in CAP 437 from UK Civil Aviation Authority, which contains

standards for offshore helicopter landing areas, there is a recommendation of not to exceed a temperature increase higher than 2ºC for helicopters operating around offshore oil and gas platforms. An important review about the smoke nuisance problem on ships was also made by Kulkarni et al (2005). They identified the down wash problem of hot air discharged from the ship's funnel affecting topside operational areas of naval ships. They summarized different investigations performed with analytical methods, CFD, and wind tunnel tests and included also a review of the evolution of the chimneys since 1930's. In addition, they indicated that modern ships with short and streamlined funnels continue presenting smoke nuisance problem.

The problems related with plumes are not new and there are a wide range of studies about them. Estimations of the final height of a plume in a stratified fluid under various conditions were already included in a previous study performed by Morton et al. (1956). Far from the chimney, the atmospheric turbulence is the dominant cause of mixing. In that situation, experimental data about the buoyant rise of chimney plumes was presented by Slawson and Csanady (1971). More specific to frigates, Baham et al. (1977) presented design techniques for ship funnels, including different guidance for selecting the proper height, shape and location of the stack, and techniques to predict the plume trajectory and temperatures. Nishiyama et al. (1990) used a simple heated two-dimensional jet injected in a cold cross flow under different blowing rates. They extracted the temperature field and jet flow patterns. König et al. (2002) published numerical simulations using k−ε turbulence model for multi-plumes and compared the results of velocity, temperature and turbulence energy fields with a single plume. They conclude that the differences were minimal at ten diameters downstream the plume source. Using numerical simulations, a jet injected vertically into a crossflow was solved and compared with particle visualizations to obtain the mechanism of the creation of the wake vortices (Muldoon et al. 2010). Two years later, Hargreaves et al. (2012) presented a numerical study with CFD for turbulent plumes and jets in order to obtain quantitative data and plume spread coefficients. They included also a sensitivity study to delimit the applicability of their simulations.

More recently, Dobrucali and Ergin (2014 & 2017) published two papers about the exhaust smoke dispersion problem for a generic frigate. They investigated numerically the effects of the operational conditions and yaw angle, velocity ratio, turbulence, buoyancy of the plume, and stack geometry. In addition to the simulations, they performed experimental trials with flow visualization tests using a 1/100 scale frigate model in wind tunnel. Using the experiments they could validate the numerical simulations and conclude that buoyancy effect increases with the exhaust gas temperature and that momentum has more effect on the plume dispersion. It is important to point that the studies are not always centered on military ships. Park et al. (2016) analyzed through CFD the influence of design parameters in the exhaust plume behavior of a container carrier and compared the results with experimental data. They tested different conditions of ship, wind angle, mast height, and chimney height.

The aim of this paper is to use Computational Fluid Dynamics (CFD) to estimate the performance losses of the engine power and thrust of a helicopter operating in the presence of frigate exhaust emissions. Using a Simplified Frigate Shape 2 (SFS2) and simulating different cases of velocities and temperatures of the outlet gases, the temperature variations along the helicopter recovery maneuver from the stern are analyzed. Section 2 defines the problem approach. In section 3, the helicopter recovery maneuver from the stern is described. Section 4 summarizes the numerical set-up used for the simulations in ANSYS Fluent, giving details of the computational domain, unstructured grid, boundary conditions and numerical scheme used for calculations. The results are displayed in section 5. The temperature variations along the maneuver for the nine cases simulated, and the related effects of engine power drop, and thrust losses are also displayed. Finally, section 6 contains conclusions extracted from the paper.

2. PROBLEM APPROACH

Helicopter recovery operations above frigates are performed during the navigation of the frigate. This means that the ship needs to exhaust gases from its engine, which are usually at high temperatures. In addition, as frigates can sail at different navigations conditions if the navigation speed of the frigate increases, the engine needs more power and will produce exhaust gases with higher flow rate, velocity, and temperature, affecting conditions downstream of the frigate, where the helicopter approaches.

Figure 1 shows a scheme of the problem described. The frigate is sailing at a cruising speed of 18 knots (9.2 m/s). Assuming also low-intensity incident wind, the relative wind simulated for the problem on the deck is $U_\infty = 10\ \mathrm{m/s}$, with a temperature of $T_\infty = 288\ \mathrm{K}$. Exhaust gases from the engine are discharged through the chimney, which is located on the frigate's superstructure. These gases are released into the atmosphere with temperature T_s and velocity V_e, which may vary depending on the sailing condition and the characteristics of the frigate propulsion plant. Both values of temperature and velocity of the gas outlet can be non-dimensionalized using two coefficients. The first one is the velocity coefficient (K), that which can be defined as,

$$K = \frac{V_e}{U_\infty} \tag{1}$$

where V_s is the smoke outlet velocity, and U_∞ is the free-stream velocity that is the composition of the atmospheric wind velocity and the frigate navigational velocity.

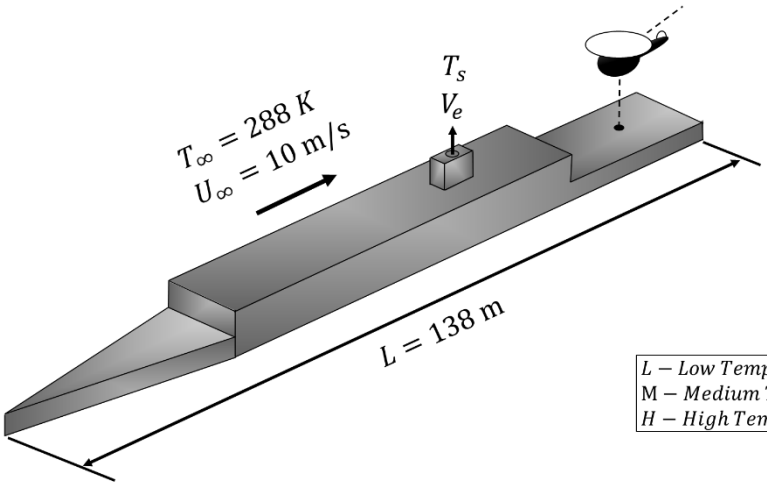

Case	K	η
L – 0.5	0.5	1.30
L – 1.0	1.0	1.30
L – 1.5	1.5	1.30
M – 0.5	0.5	1.50
M – 1.0	1.0	1.50
M – 1.5	1.5	1.50
H – 0.5	0.5	1.70
H – 1.0	1.0	1.70
H – 1.5	1.5	1.70

$L - Low\ Temperature$
$M - Medium\ Temperature$
$H - High\ Temperature$

$K = \frac{V_e}{U_\infty}$

$\eta = \frac{T_s - T_\infty}{T_\infty}$

Figure 1. Parameters of the exhaust gases problem.

The second one is the non-dimensional temperature difference (η),

$$\eta = \frac{T_s - T_\infty}{\mathrm{T}_\infty} \tag{2}$$

where $T_\infty = 288$ K is the temperature of the incident airflow and T_s is the temperature of the frigate exhaustions gases.

As a simple frigate model is used for simulations, no propulsion plant data are available. Then, a typical range of velocity and temperature coefficients will be analyzed to characterize their effects on the temperatures of the frigate wake. Specifically, figure 1 shows the 9 combinations of velocity coefficients (K) and temperature coefficients (η) tested. The nomenclature of each case contains a letter (L, M, and H) that refers to the temperature of gases outlet (low, medium, and high), and the number from 0.5 to 1.5 refers to the velocity coefficient of the outlet of the gases. For example, M – 1.5 means a case with medium temperature ($\eta = 1.50$) and high velocity coefficient ($K = 1.5$).

3. HELICOPTER RECOVERY MANEUVER

Helicopter recovery maneuvers on frigates can be performed using different approaches. One of the most common approaches is shown in figure 2 (Tušl et al., 2020). It is a recovery maneuver performed from the stern and with the helicopter always contained in the centerline plane of the frigate. The procedure starts when the helicopter is far from the frigate (1) and the pilot has to search for external reference points. Then, the helicopter descents following a flight path (2) and follows it towards the ship deck, switching to a predominantly external visual flight (3). Next step is to enter above the flight deck and align above the touchdown circle (4), hovering with a closure rate equal to zero (5), in order to descend vertically to the ship deck (6).

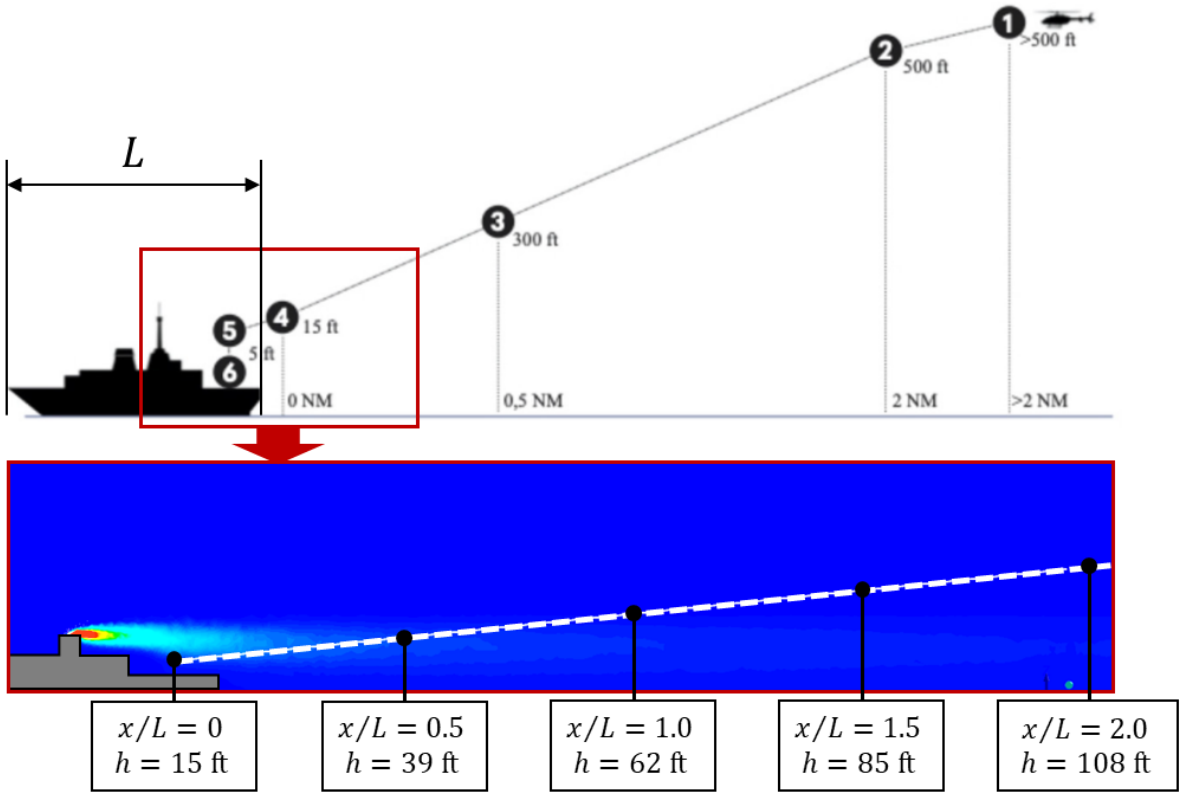

Figure 2. Helicopter trajectory during the recovery maneuver.

The most affected phases by the high temperature outlet gases from the frigate, and which will be analyzed in detail with the results of the simulations, are between phases 3 and 6. Figure 2 shows in detail with a white dotted line the final phase of the helicopter trajectory during the recovery maneuver. The trajectory also have different points marked with the altitude in feet at different distances in frigate lengths (L) to the flight deck center.

4. NUMERICAL SET-UP

The Simple Frigate Shape 2 was proposed by a ship air wake modeling working group within the Technical co-operation Program (TTCP) to standardize a frigate model for aerodynamic research (Bardera, 2014, Zan, 2000, Yuan, 2016, 2018).

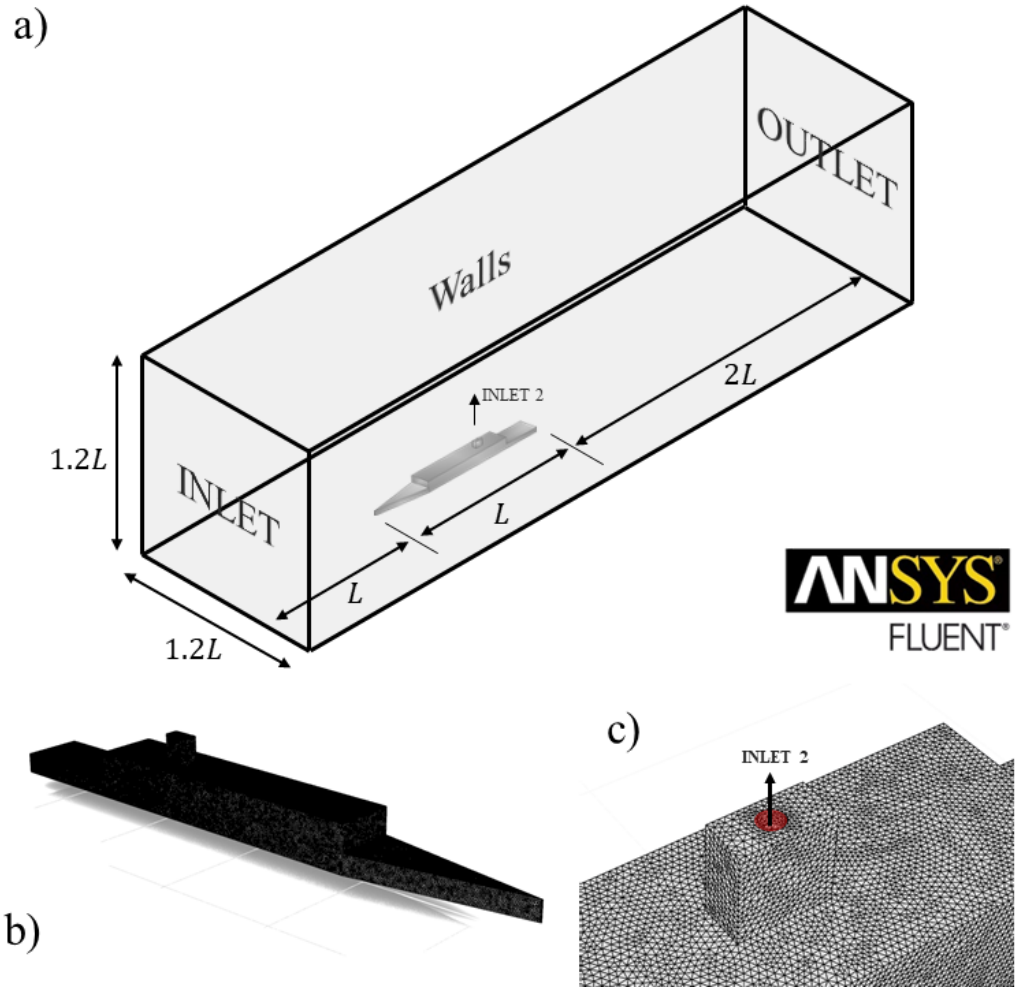

Figure 3. a) Dimensions of the computational domain. b) Mesh refinement above the SFS surface c) Detail view of the stack gases outlet (inlet 2) of the SFS.

The full scale SFS2 has $L = 138$ m of length. Its geometry represents the above waterline parts of a frigate: the hull, the bow, the superstructure, the stack gases outlet and the helicopter flight deck at the

stern. The location of the flight deck behind superstructure, is the cause of the presence of low velocities areas and detached flows that can affect the safety of helicopter recovery maneuvers. As an alternative to the aerodynamic problem, this study aims to analyze the effect on the helicopter of the outflow of gases at high temperatures through the chimneys of the ship.

The computational domain is displayed in figure 3 a. It was created using Design Modeler package of ANSYS, from an "*.igs"* file extension created with 3D computer aid design software. Upstream the frigate model there is a distance L to the inlet with $U_\infty = 10\,\mathrm{m/s}$ and $T_\infty = 288\,\mathrm{K}$ of boundary condition. Wall conditions with standard wall functions are applied on the surfaces, lateral and upper limits of the domain at $1.2L$ distances from the model. The outlet condition is placed at a distance $2L$ downstream of the model. To simulate the exhaust gases at high temperature from the frigate, another inlet condition was imposed at the chimney outlet (inlet 2, figure 3 c). The velocities imposed from this inlet were chosen at 5, 10 and 15 m/s to simulate $K = 0.5$, 1.0 and 1.5, and the temperatures of $T_{inlet2} =$ 673, 723, and 773 K to simulate $\eta = 1.30$, 1.50 and 1.70, respectively.

The computational domain was filled using unstructured grid. The maximum size of the elements far from the surfaces of the frigate was 2 m. To improve the results, the density of mesh elements is much higher near the frigate surfaces. Sizing restrictions were imposed on all the surfaces of the frigate and the near field (figure 3 b, and c), with a maximum size of these elements of 0.4 m. This configuration resulted in a mesh with a total of 4.2 million of elements.

The solver used was Fluent version 2021 R1, and 4 solver processors of 3.20 GHz working in parallel. The turbulence model used for calculations was the two equation viscous model SST $K-\omega$. For temperature calculations the energy equation had to be included in the simulations. Finally, each case simulated was initialized using inlet conditions. The solutions were founded using a coupled scheme with least squares cell gradient based spatial discretization, and second order upwind scheme with double precision for convergence. In general, the solution converged with less than 500 iterations with a computational time of between 1.5 and 3 hours. Once the simulations converged, the results of temperature were extracted in temperature contours on the centerline plane of the frigate and in plots with temperature along the flight path of the helicopter during the recovery maneuver that will be shown in the next section.

5. RESULTS

5.1 Temperature contours

This section shows temperature contours extracted on the centerline plane of the frigate during the nine conditions simulated. All contours of figure 4 have the recovery path of the helicopter marked with a white line. The contours have been grouped for low (L, $\eta = 1.30$), medium (M, $\eta = 1.50$) and high (H, $\eta = 1.70$) outlet temperatures, for the different velocity coefficients (K) simulated. In order to compare the results, similar color scale is used in all of them, with a minimum value of 288 K and red contours for higher temperatures than 330 K. In all cases it can be observed that the high temperature gases are deflected downstream of the frigate due to its interaction with the free-stream velocity (U_∞). In addition, the temperature of the gases drops rapidly, reaching values below 310 K (green contours) above the flight deck, and continue to drop to around 300 K (light blue contours) as these gases approach the helicopter trajectory.

The effect of varying the outlet gases temperature (η) seems little noticeable. For the same value of K, the different cases of η does not cause large changes in the temperature field. It appears that the temperature of the gases dissipates rapidly with the large amount of incident flow at $U_\infty = 10$ m/s. However, varying the outlet velocities (K) has much more significant effects. The high temperature zones (> 330 K) extends to a greater area of the contours as the value of K increases. And the temperatures in the positions where the helicopter operates during the maneuver are clearly higher as the value of K increases.

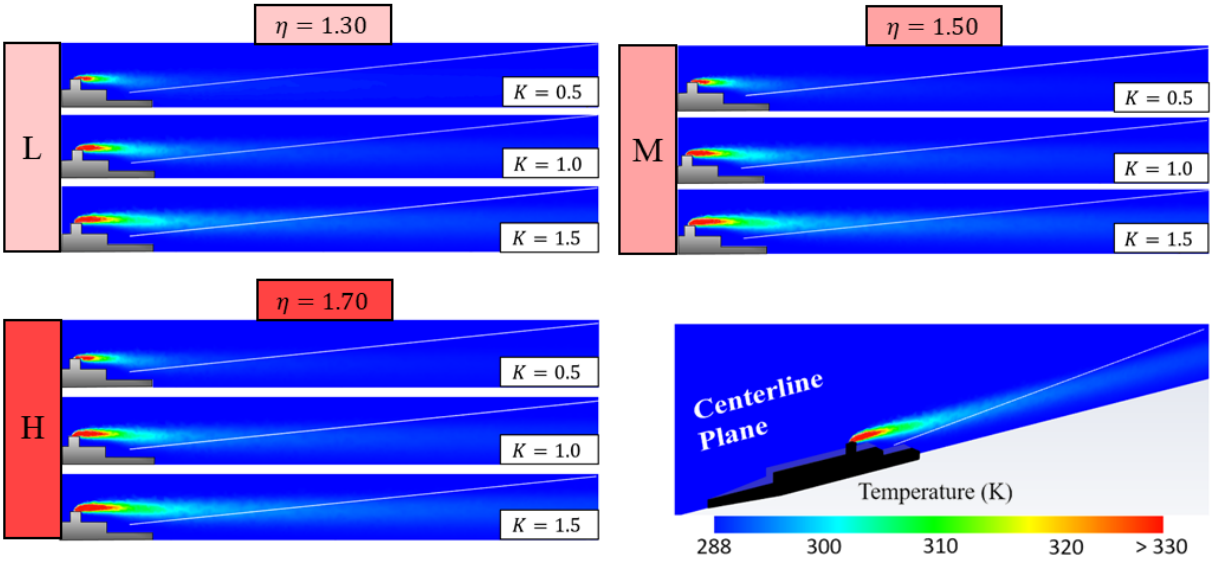

Figure 4. Temperature contours for the different cases tested on the centerline plane of the frigate.

5.2 Temperature profiles

From the results shown in the temperature contours of the previous section, it is possible to obtain the temperature variations along the helicopter recovery maneuver. In figure 5, the temperature profiles along the flight path are displayed from the nine cases simulated. The horizontal axis shows the distance of the helicopter to the final landing point in frigate lengths (x/L). The vertical axis shows the temperatures in K, and also in non-dimensional value, expressed as the percentage increase in temperature with respect to the ambient temperature,

$$\theta(\%) = \frac{T_x - T_\infty}{\mathrm{T}_\infty} \times 100 \tag{3}$$

The color of the curves indicates the output gases temperature, being red for high temperature (H), orange for intermediate (M) and green for low temperature (L). The trace of the lines indicates the velocity coefficient: $K = 0.5$ represented with thick dashed lines, $K = 1.0$ for thin dashed lines and $K = 1.5$ for the dotted plots. As a complement to the plot, Table 1 shows the maximum temperature values registered along the recovery path in each case and ordered from highest to lowest. This value is shown in absolute value in K, as a difference with the ambient temperature ($\Delta T = T_x - T_\infty$), and in non-dimensional value as a percentage variation with respect to the ambient temperature (θ). Finally, the position in the maneuver at which the temperature is maximum is also displayed for each case.

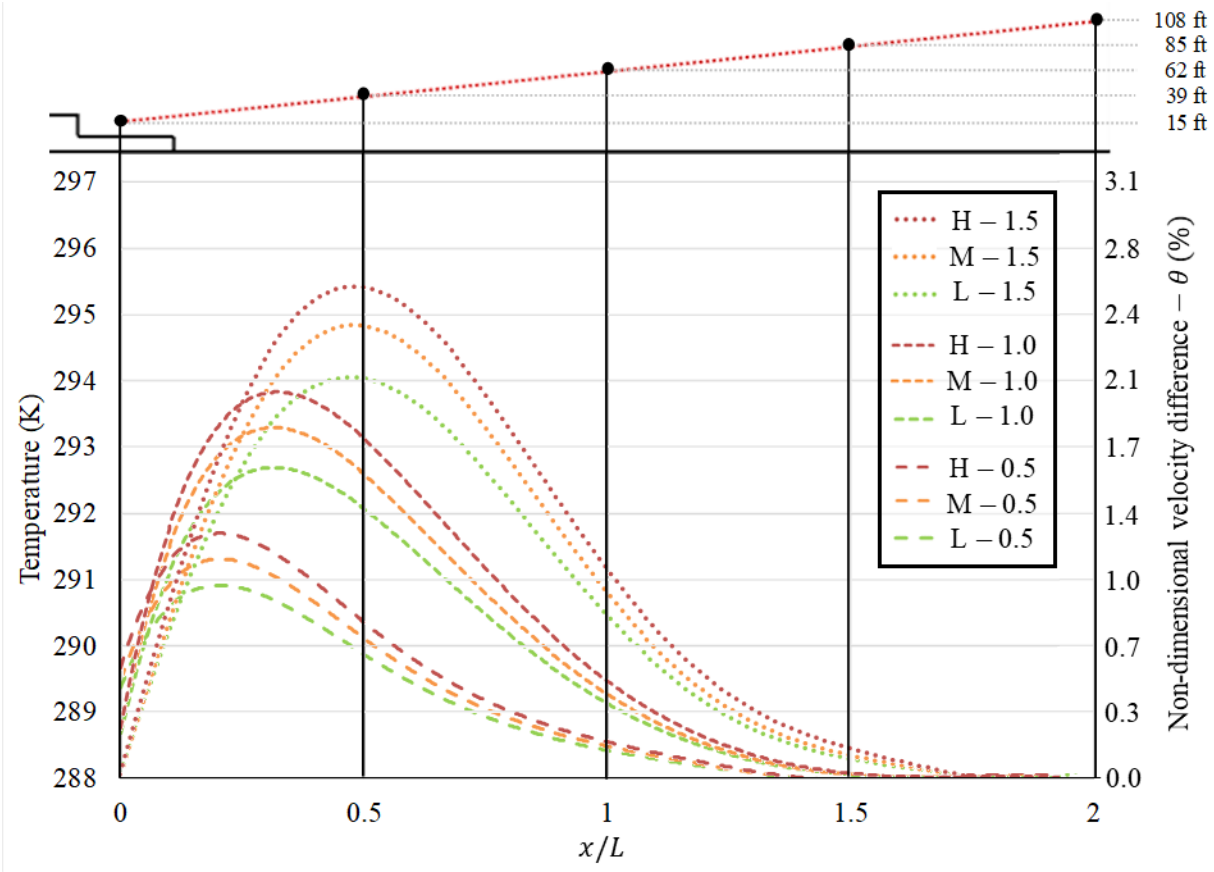

Figure 5. Temperature variations along the helicopter recovery maneuver path for the nine cases tested.

From the plots and numerical values presented, it is possible to draw a series of conclusions. Among the two parameters tested, the velocity coefficient (K) has the greatest effect on the increase in temperature.

When the value of K is low, the maximum temperatures are reached close to the end point of the maneuver ($x/L = 0.16$). If the velocities are higher ($K = 1$), the highest temperatures are reached at the point $x/L = 0.29$. Finally, for the highest velocity coefficient tested ($K = 1.5$), the maximum temperatures are reached around point $x/L = 0.45$.

The change in the chimney temperature outlet has a smaller effect on the curves. If the gas outlet temperatures increase from the L case ($\eta = 1.30$) to the M case ($\eta = 1.5$), the maximum temperatures along the flight path only increase by 0.5 % when $K = 0.5$, by 0.6 % when $K = 1.0$ and by up to 0.8 % when $K = 1.5$. In the same way, a further temperature increase for M cases and H cases causes increases of 0.4 %, 0.6 %, and 0.7 % for the cases of $K = 0.5$, 1.0, and 1.5, respectively.

5.3 Helicopter performance variations

Once the temperature profiles have been obtained throughout the helicopter recovery maneuver, an estimation of its performance drop can be made. Most helicopters have a turbine engine that powers the

main rotor. This engine takes air from the outside. A rise in the air temperature causes a decrease in air density, resulting in a reduction in the performance of the helicopter engine, figure 6.

Table 1. Maximum temperatures reached along the recovery maneuver.

Case	η	K	T_{max}	ΔT_{max}	$\theta_{max}(\%)$	$(x/L)\,T_{max}$
H - 1.5	1.70	1.5	295.8 K	7.8	2.7	0.45
M - 1.5	1.50	1.5	295.1 K	7.1	2.5	0.45
L - 1.5	1.30	1.5	294.3 K	6.3	2.2	0.45
H - 1.0	1.70	1.0	294.1 K	6.1	2.1	0.29
M - 1.0	1.50	1.0	293.5 K	5.5	1.9	0.29
L - 1.0	1.30	1.0	292.9 K	4.9	1.7	0.29
H-0.5	1.70	0.5	292.0 K	4.0	1.4	0.16
M-0.5	1.50	0.5	291.6 K	3.6	1.2	0.16
L-0.5	1.30	0.5	291.1 K	3.1	1.1	0.16

The power losses caused by temperature change can be quantified from the following expression,

$$\frac{EP_2}{EP_1} = \frac{EP_1 + \Delta EP}{EP_1} = \frac{P_2}{P_1} = \left(\frac{\rho_2}{\rho_1}\right)^{\mathrm{m}} = \left(\frac{T_1}{T_2}\right)^{\mathrm{m}} = \left(\frac{T_1}{T_1 + \Delta T}\right)^{\mathrm{m}} \tag{4}$$

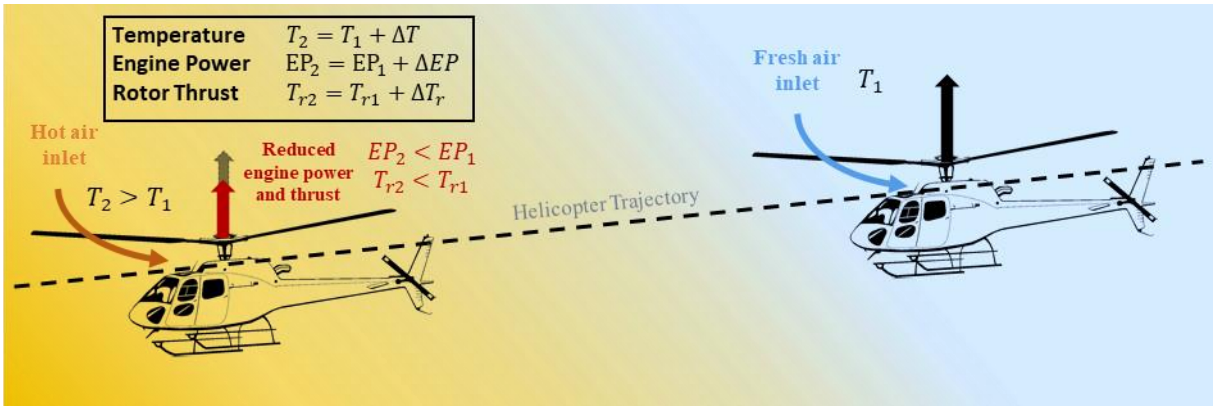

Figure 6. Helicopter performances variation with an increase of air temperature inlet.

where EP are the engine power, P is the air pressure, ρ is the air density, T is the air temperature, m is a constant value that depends on the helicopter engine (usually m ~ 0.85), and the subscript indicates the helicopter position 1 and 2, which results in a change of the environmental conditions. Expression (4) can be simplified to obtain the engine power variations experienced (ΔEP) as a function of the temperature variations (ΔT),

$$\frac{\Delta EP}{EP_1} = \left(\frac{1}{1 + \Delta \mathrm{T}/\mathrm{T}_1}\right)^{\mathrm{m}} - 1 \tag{5}$$

As a consequence, the lower air density causes a reduction in the thrust generated by its main rotor.

Additionally, during hovering flight, the rotor thrust (T_r) can be calculated as,

$$T_r = \dot{m}\mathrm{W} = \dot{m}(2\mathrm{V_i}) = 2\rho \mathrm{V_i^2 A} \tag{6}$$

where $\dot{m}$ is the mass flow rate, W is the vertical speed, V_i is the induced velocity at the rotor plane, and A is the main rotor surface. The necessary engine power during hovering flight is,

$$EP = T_r V_i = \frac{\mathrm{T_r}^{3/2}}{\sqrt{2\rho A}} \tag{6}$$

The thrust ratio at two points with different environmental conditions will be,

$$\frac{T_{r2}}{T_{r1}} = \frac{T_{r1} + \Delta T_r}{T_{r1}} = \left(\frac{EP_2}{EP_1}\right)^{2/3} \left(\frac{\rho_2}{\rho_1}\right)^{1/3} \tag{7}$$

From where it can be deduced that the thrust variation (ΔT_r) due to the temperature change (ΔT) is,

$$\frac{\Delta T_r}{T_{r1}} = \left(\frac{1}{1 + \Delta \mathrm{T}/\mathrm{T}_1}\right)^{\frac{1}{3}(1+2\mathrm{m})} - 1 \tag{8}$$

To summarize, a change in temperature (ΔT) causes a loss in the helicopter engine power (5), and a loss in main rotor thrust (8). Using these expressions for the nine simulations performed, figure 7 contains the thrust losses during the helicopter recovery maneuver flight path for the nine cases simulated. In table 2, the maximal engine power and thrust losses reached in each case are also displayed.

As the drop in the engine performance and the helicopter rotor thrust are related to the temperature increase, figure 7 has a similar trend that the temperature plots displayed in figure 5. Thus, when the K value is low ($K = 0.5$), temperature gradients are also lower and the thrust losses are less important. As the value of K increases to moderate or high values ($K = 1.0$, and 1.5), thrust losses can reach up to 2.36 %. Similar to temperature variations, increasing outlet temperature has a reduced effect on helicopter performance. As an example, for the same velocity coefficient ($K = 1.5$), changing the outlet temperatures (L, M, and H) only affects by deteriorating the performance by 0.18 to 0.25 %.

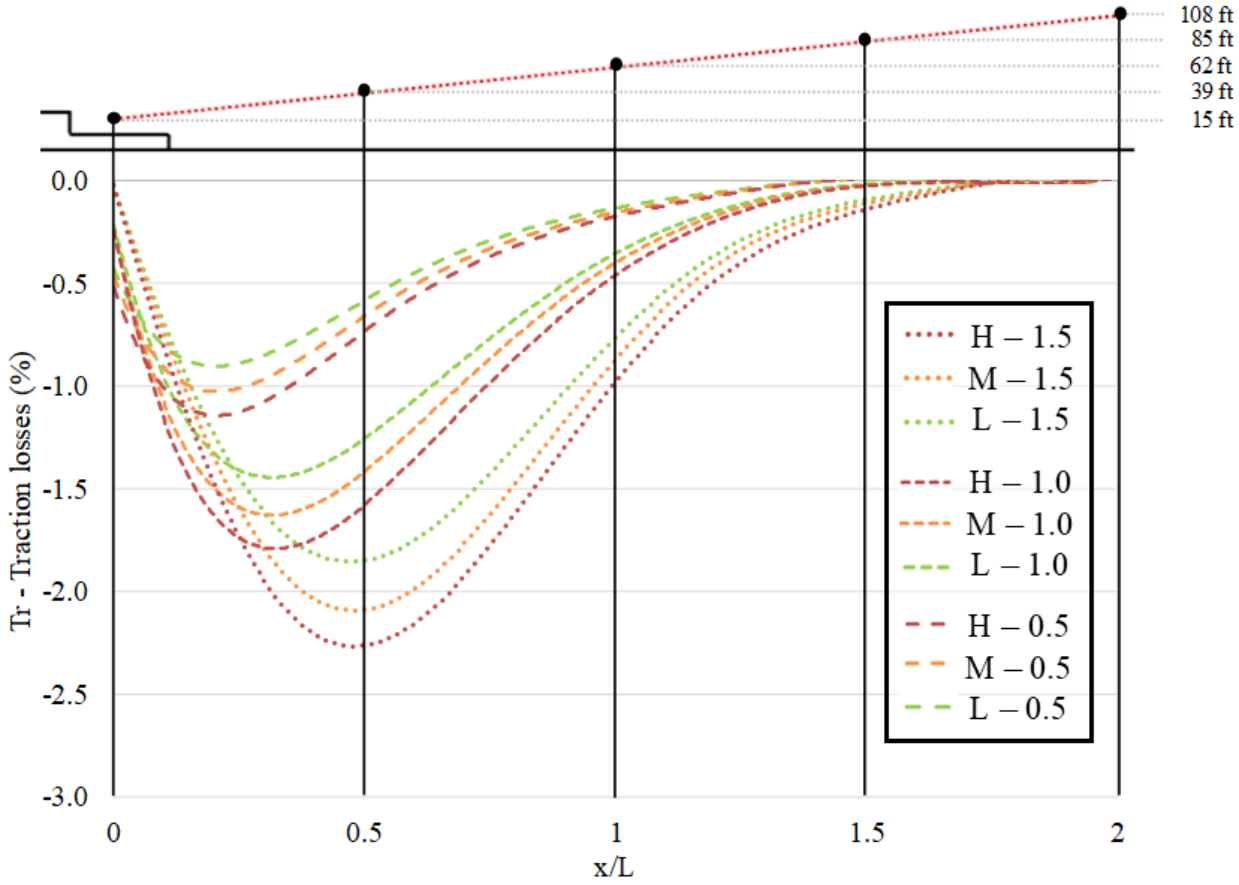

Figure 7. Thrust losses along the helicopter recovery maneuver path for the nine cases tested.

Figure 8 graphically summarizes the results contained in Table 2. It is again observed that the effect on helicopter performance is greater when changing the jet exit velocities (K) than when increasing the exit temperature.

6. CONCLUSIONS

The engine of a frigate generates high-temperature gases that are dispersed to the atmosphere through its chimney. These gases can interfere with the electronical devices of the ship and the helicopter's performance when operating above the flight deck. CFD has been used in this paper as a tool to obtain the temperature variations experienced by the helicopter during the approach trajectory and recovery maneuver on a frigate. The simulated trajectory from the stern is always contained in the centerline of the frigate, with a linear descent to the flight deck. The gas outlet conditions have been varied for 3 velocity coefficients ($K = 0.5, 1.0$, and 1.5) and for 3 different outlet temperatures ($\eta = 1.30, 1.50$, and 1.70).

The results have shown maximum temperature increases between 3 and 8 K, resulting in a reduction of the helicopter engine power between 0.9 % to 2.2 % and total thrust losses between 1 and 2.4 %, depending on the temperature and flow conditions of the gas jet. In addition, the effect of the gas outlet

flow rate (K) on the helicopter inlet temperatures and performances is always greater than changing the frigate gas outlet temperatures (η).

Table 2. Maximum engine Power (EP) and Thrust (Tr) losses during recovery maneuver

Case	η	K	T_{max}	EP (%)	T_r(%)
H - 1.5	1.70	1.5	295.8 K	-2.23	-2.36
M - 1.5	1.50	1.5	295.1 K	-2.06	-2.18
L - 1.5	1.30	1.5	294.3 K	-1.83	-1.93
H - 1.0	1.70	1.0	294.1 K	-1.75	-1.86
M - 1.0	1.50	1.0	293.5 K	-1.59	-1.69
L - 1.0	1.30	1.0	292.9 K	-1.41	-1.50
H-0.5	1.70	0.5	292.0	-1.16	-1.23
M-0.5	1.50	0.5	291.6	-1.04	-1.10
L-0.5	1.30	0.5	291.1	-0.92	-0.97

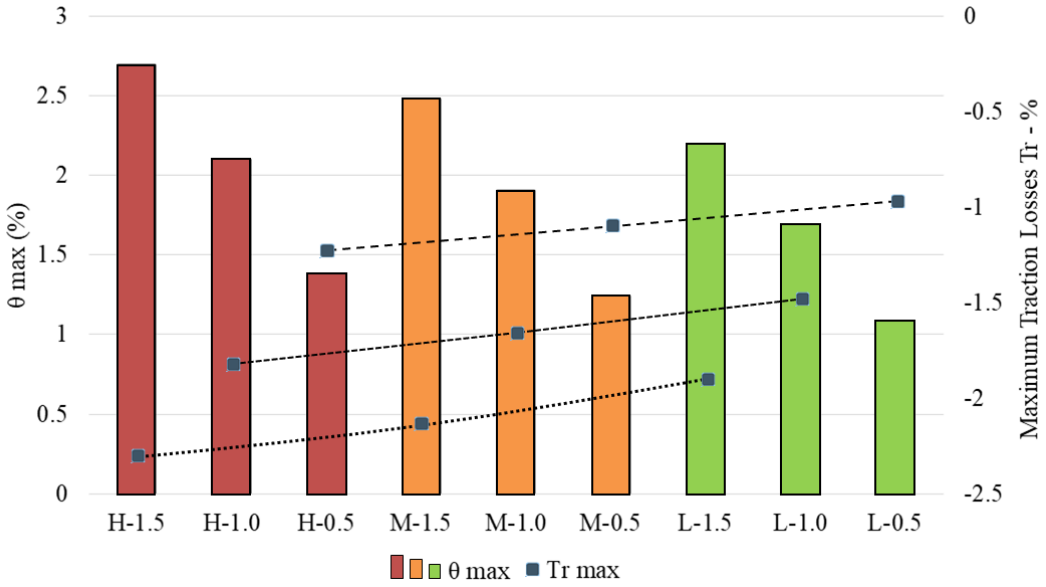

Figure 8. Maximum temperature increment (θ_{max}) and thrust losses (T_r).

The temperature increase seems low, but there is a security recommendation of not to exceed a temperature increase higher than 2ºC for helicopters operating around offshore oil and gas platforms. Then, despite this study has been applied to a simplified frigate mode, temperature fields around the new frigates design should be analyzed in depth to ensure safe operation and avoid abrupt thrust changes during the helicopter recovery maneuver over the frigate.

ACKNOWLEDGEMENTS

The authors would like to thank the staff of the Experimental Aerodynamics department of INTA who participated in the tests presented in this paper. This study is included in the "Termofluidodinámica" program 464A 64 1999 14 205 0005 of the Spanish Ministry of Defense with INTA internal code IDATEC S.IGB21001.

REFERENCES

Baham Gary, J.; Mc Cullum, D. Stack (1977) Stack Design technology for Naval and Merchant Ships. Trans SNAME, 85, 324-349.

Bardera, R. (2014). Experimental Investigation of the Flow on a Simple Frigate Shape (SFS). The Scientific World Journal, 2014:1-8.

CAP 437. Standards for offshore helicopter landing areas. Safety Regulation Group. UK Civil Aviation Authority.

Dobrucali, E. (2012) "A brief review on examination of exhaust gas dispersion on marine ships". Journal of Marine Science and Engineering, 8 (2), pp. 46-56.

Dobrucali, E. and Ergin, S. (2017) "An investigation of exhaust smoke dispersion for a generic frigate by numerical analysis and experiment," Proceedings of the Institution of Mechanical Engineers, Part M: Journal of Engineering for the Maritime Environment, 233(1), pp. 310–324. https://doi.org/10.1177/1475090217742240

Ergin, S. and Dobrucalı, E. (2014) "Numerical modeling of exhaust smoke dispersion for a generic frigate and comparisons with experiments," Journal of Marine Science and Application, 13(2), pp. 206–211. https://doi.org/10.1007/s11804-014-1246-x.

Hargreaves, D.M., Scase, M.M. and Evans, I. (2012) "A simplified computational analysis of turbulent plumes and Jets," Environmental Fluid Mechanics, 12(6), pp. 555–578. https://doi.org/10.1007/s10652-012-9250-7.

König, C.S. and Mokhtarzadeh-Dehghan, M.R. (2002) "Numerical study of buoyant plumes from a multi-flue chimney released into an atmospheric boundary layer," Atmospheric Environment, 36(24), pp. 3951–3962. Available at: https://doi.org/10.1016/s1352-2310(02)00310-2.

Kulkarni, P.R., Singh, S.N. and Seshadri, V. (2005) "The smoke nuisance problem on ships - A Review," The International Journal of Maritime Engineering, 147(a2), p. 15. https://doi.org/10.3940/rina.ijme.2005.a2.050257.

Muldoon, F. and Acharya, S. (2010) “Direct numerical simulation of pulsed jets-in-crossflow,” Computers & Fluids, 39(10), pp. 1745–1773. https://doi.org/10.1016/j.compfluid.2010.04.008.

Morton, B.R.; Taylor G.I.; Turner, J.S. (1956) “Turbulent gravitational convection from maintained and instantaneous sources” Proceedings of the Royal Society of London. Series A. Mathematical and Physical Sciences, 234(1196), pp. 1–23. https://doi.org/10.1098/rspa.1956.0011.

Nishiyama, H. et al. (1990) “Temperature field of a slightly heated jet in a cross flow,” Wärme- und Stoffübertragung, 25(6), pp. 369–375. https://doi.org/10.1007/bf01811561.

Park, S., Yang, J. and Rhee, S.H. (2016) “Parametric study on ship’s exhaust-gas behavior using computational fluid dynamics,” Engineering Applications of Computational Fluid Mechanics, 11(1), pp. 159–171. https://doi.org/10.1080/19942060.2016.1260057

Scott, P., White, M.D., Owen, I., (2015) “Unsteady CFD modelling of ship engine exhaust gases and over-deck air temperatures, and the implications for maritime helicopter operations”, American Helicopter Society, 71st Annual Forum, Virginia Beach, VA, May 5-7, 2015.

Slawson, P.R. and Csanady, G.T. (1971) “The effect of atmospheric conditions on plume rise,” Journal of Fluid Mechanics, 47(1), pp. 33–49. Available at: https://doi.org/10.1017/s0022112071000910.

Tušl, M., Rainieri, G., Fraboni, F., De Angelis, M., Depolo, M., Pietrantoni, L., Pingitore, A. (2020). Helicopter pilots’ tasks, subjective workload, and the role of external visual cues during shipboard landing. Journal of Cognitive Engineering and Decision Making, 14(3), 242–257. https://doi.org/10.1177/1555343420948720

Yuan W., R. Lee and A. Wall (2016). Simulation of Unsteady Ship Airwakes Using Openfoam. In : 30th Congress of the International Council of the Aeronautical Sciences. DCC, Daejeon, Korea: September 25-30.

Yuan, W., A. Wall and R. Lee. (2018). Combined numerical and experimental simulations of unsteady ship airwakes. Computers & Fluids, 172: 29-53.

Zan, S. J. (2000). Surface Flow Topology for a Simple Frigate Shape. Canadian Aeronautics and Space Journal. 47:33-43.